

# SCIENTIFIC REPORTS

OPEN

## Central insulin action induces activation of paraventricular oxytocin neurons to release oxytocin into circulation

Boyang Zhang<sup>1</sup>, Masanori Nakata<sup>1,2</sup>, Jun Nakae<sup>3</sup>, Wataru Ogawa<sup>4</sup> & Toshihiko Yada<sup>1,5</sup>

Oxytocin neurons in the paraventricular nucleus (PVN) of hypothalamus regulate energy metabolism and reproduction. Plasma oxytocin concentration is reduced in obese subjects with insulin resistance. These findings prompted us to hypothesize that insulin serves to promote oxytocin release. This study examined whether insulin activates oxytocin neurons in the PVN, and explored the underlying signaling. We generated the mice deficient of 3-phosphoinositide-dependent protein kinase-1 (PDK1), a major signaling molecule particularly for insulin, specifically in oxytocin neurons (*Oxy Pdk1* KO). Insulin increased cytosolic calcium concentration ( $[Ca^{2+}]_i$ ) in oxytocin neurons with larger ( $\geq 25 \mu\text{m}$ ) and smaller ( $< 25 \mu\text{m}$ ) diameters isolated from PVN in C57BL/6 mice. In PDK1 *Oxy Pdk1* KO mice, in contrast, this effect of insulin to increase  $[Ca^{2+}]_i$  was markedly diminished in the larger-sized oxytocin neurons, while it was intact in the smaller-sized oxytocin neurons. Furthermore, intracerebroventricular insulin administration induced oxytocin release into plasma in *Oxy Cre* but not *Oxy Pdk1* KO mice. These results demonstrate that insulin PDK1-dependently preferentially activates PVN magnocellular oxytocin neurons to release oxytocin into circulation, possibly serving as a mechanism for the interaction between metabolism and perinatal functions.

Insulin has various effects in multiple tissues, including stimulation of glucose uptake in skeletal muscle and adipose tissue and suppression of gluconeogenesis and glycogenolysis in the liver, thereby lowering the blood glucose level. In addition to the peripheral action, insulin is known to lower blood glucose via central action<sup>1,2</sup>. Insulin receptor is widely expressed in the brain, including hypothalamus, olfactory bulb, hippocampus, cerebral cortex and cerebellum<sup>3</sup>. A knockout of insulin receptor in neuronal tissue (NIRKO) showed increases in body weight, white adipose tissue, and serum triglycerides, and these changes were more pronounced in females<sup>4</sup>. Furthermore, NIRKO mice of both sexes showed reduced fertility. Diabetes mellitus is known to increase the frequency of maternal complications during perinatal periods in pregnancies. These findings have demonstrated the importance of insulin in maintaining reproduction and perinatal functions. However, the effect of central insulin on the hormone that regulates reproduction and perinatal functions remains unclear.

Oxytocin, a neuropeptide with 9 amino acid residues, is produced by two types of oxytocin neurons in the hypothalamus; the magnocellular neurons in the paraventricular nucleus (PVN) and supraoptic nucleus (SON), and the parvocellular neurons in PVN. The parvocellular oxytocin neurons in PVN project to the hypothalamus, limbic system and brain stem, and are involved in sexual behavior, social adaptive behavior, feeding behavior, learning and memory<sup>5-10</sup>. The magnocellular oxytocin neurons release oxytocin into the blood vessels from their axon terminals in the posterior pituitary gland, and thereby elicit uterine contraction and milk ejection,

<sup>1</sup>Department of Physiology, Division of Integrative Physiology, Faculty of Medicine, Jichi Medical University, 3311-1 Yakushiji, Shimotsuke, Tochigi, 329-0498, Japan. <sup>2</sup>Department of Physiology, Faculty of Medicine, Wakayama Medical University School of Medicine, 641-8509, Kimiidera 811-1, Wakayama, Wakayama, Japan. <sup>3</sup>Frontier Medicine on Metabolic Syndrome, Division of Endocrinology, Metabolism and Nephrology, Department of Internal Medicine, Keio University School of Medicine, Tokyo, Japan. <sup>4</sup>Department of Internal Medicine, Division of Diabetes and Endocrinology, Kobe University Graduate School of Medicine, Kobe, Japan. <sup>5</sup>Kansai Electric Power Medical Research Institute, 1-5-6 Minatojima-minamimachi, Chuo-ku, Kobe, 650-0047, Japan. Correspondence and requests for materials should be addressed to M.N. (email: [mnakata@wakayama-med.ac.jp](mailto:mnakata@wakayama-med.ac.jp)) or T.Y. (email: [toshihiko.yada@kepmri.org](mailto:toshihiko.yada@kepmri.org))

contributing to reproduction and perinatal functions. Recently, oxytocin has been shown to play an important role in maintenance of metabolism and energy balance<sup>11–15</sup>. Inversely, decreased plasma level of oxytocin in obese patients was reported<sup>16</sup>. These findings prompted us to hypothesize that insulin serves to promote oxytocin release. In this study, we aimed to clarify whether insulin activates oxytocin neurons in the PVN and, if so, to explore the underlying signaling pathway.

## Methods

**Animals.** Male C57BL/6 mice (SLC, Hamamatsu, Japan) were single-housed for *in vivo* experiments and group-housed for Ca<sup>2+</sup> imaging under a 12-h light/dark cycle condition (7:30 light on). Food (Standard animal chow CE-2; CLEA, Osaka, Japan) and water were available *ad libitum* except particular experiments performed under fasted conditions.

We generated oxytocin neuron-specific 3-phosphoinositide-dependent protein kinase-1 (PDK1) knockout (*Oxy Pdk1 KO*) mice by mating Oxytocin-Ires-Cre knock-in mice (*Oxy Cre*) (a generous gift from Dr. Bradford B Lowell, Beth Israel Deaconess Medical Center/Harvard Medical School) with *Pdk1*-floxed mouse with loxP sites flanking exons 3 and 4<sup>2,15</sup>. All mice were genotyped by polymerase chain reaction (PCR) amplification of genomic DNA isolated from tail tips. Both *Oxy Cre* mice and *Oxy Pdk1KO* mice were maintained in the same conditions as for C57BL/6 mice. Male mice were used for the experiment. All animal procedures were conducted in compliance with protocols approved by Jichi Medical University Animal Care and Use Committee.

**Intracerebroventricular (ICV) injection.** Mice aged 9 weeks were anesthetized by intraperitoneal (ip) injection of pentobarbitone (50 mg/kg, ip). A guide cannula (ICM-23G09; Intermedical, Osaka, Japan) was inserted into lateral ventricle (LV) with the tip located at 0.5 mm caudal, 0.1 mm lateral to the bregma, and 2.2 mm below the skull. Mice were allowed to recover from surgery for at least one week before being subjected to tests. Intraventricular administration of human insulin (100 μU/2 μl) was performed immediately within 30 minutes before the dark period after fasting for 10 hours. At 30 minutes after insulin injection, trunk blood was collected immediately after decapitation without anesthesia. Plasma concentrations of oxytocin (Phoenix Pharmaceutical, Inc, Burlingame, CA) were measured with enzyme immunoassay method according to the instruction.

**Immunohistochemistry for *pdk1* and oxytocin.** Mice were deeply anesthetized with 2,2,2-tribromoethanol and perfused transcardially with 4% paraformaldehyde in 0.1 M phosphate buffer (PB) for 20 min. The brains were removed and subjected to immunohistochemistry. Coronal sections (40 μm) of the hypothalamus were cut using a freezing microtome and collected at 120 μm intervals. The brain was immunostained for PDK1 using rabbit anti-PDK1 antibody (ab52893; Abcam, Cambridge; 1:1000 dilution) and for oxytocin using mouse anti-oxytocin antibody (MAB5296; Millipore, Billerica, MA, 1:1000). Alexa fluor 488 goat anti-rabbit (Life Technologies, Carlsbad, CA; 1:500) and Alexa fluor 594 goat anti-mouse (Life Technologies, Carlsbad, CA; 1:500) were used as the secondary antibodies for PDK1 and oxytocin, respectively. The confocal fluorescence images for PDK1 and oxytocin were acquired using Olympus FV1000 confocal laser-scanning microscope (Olympus, Tokyo, Japan).

**Immunohistochemistry for c-Fos and oxytocin.** At 90 minutes after LV injection of insulin or vehicle, mouse coronal sections with 40 μm thickness were cut with a freezing microtome and collected at 160 μm intervals. Sections were rinsed in phosphate buffered saline (PBS) and then incubated in 0.3% H<sub>2</sub>O<sub>2</sub> for 20 min. After rinsing, sections were blocked with 2% bovine serum albumin and 2% normal goat serum for 30 min and incubated with rabbit anti-c-Fos antibody (sc-52, Santa Cruz, 1:5000) overnight at 4 °C. Then the sections were rinsed and incubated with biotinylated goat anti-rabbit IgG for 30 min. After rinsing, sections were incubated with avidin-biotin complex (ABC) reagent for 30 min (Vector Laboratories; 1:500). After rinsing in PBS, color was developed with a nickel-diaminobenzidine (DAB) solution (0.3% nickel ammonium sulfate, 0.02% DAB, and 0.005% H<sub>2</sub>O<sub>2</sub> in 0.05 M Tris buffer) for 5 min. For double-labeling immunohistochemistry for c-Fos and oxytocin, the process of oxytocin staining was added. After rinsing in PBS, sections were treated with an avidin and biotin blocking solution (Vector Laboratories) and then incubated with mouse anti-oxytocin antibody (Ab2078; Abcam, Cambridge, 1:1000) diluted in a blocking solution overnight at 4 °C. After rinsing, sections were incubated with biotinylated horse anti-mouse IgG antibody for 30 min and incubated in ABC reagent for 30 min. Then the sections were rinsed in PBS and Tris buffer, and color was developed with a DAB solution (0.02% DAB and 0.005% H<sub>2</sub>O<sub>2</sub> in Tris buffer). Slices were then rinsed, mounted on slides, and coverslipped with Entellan new (Merck, Darmstadt, Germany).

**Measurement of cytosolic calcium concentration ([Ca<sup>2+</sup>]<sub>i</sub>).** Single neurons were isolated from mice aged 5–6 weeks. Briefly, brain slices containing the entire PVN were prepared and the PVN was excised from the left and right sides. The dissected tissues were washed with 10 mM HEPES-buffered Krebs-Ringer bicarbonate buffer (HKRB) containing 1 mM glucose. They were then incubated in 10 mM HKRB containing 1 mM glucose, 20 U/ml papain (Sigma Chemical Co., St. Louis, MO), 0.015 mg/ml deoxyribonuclease, 0.75 mg/ml BSA, and 1 mM cysteine for 15 min at 36 °C in a shaking water bath, followed by gentle mechanical trituration for 5–10 min. After trituration, the cell suspension was centrifuged at 100 g for 5 min. The pellet was resuspended in HKRB. The single neurons obtained were distributed onto coverslips and incubated in the humidified chamber at 30 °C for 30 min and then at 25 °C for up to 6 h until use. In previous electrophysiological study of the neurons in paraventricular nucleus, the cells with cellbody >25 μm formed a small population and were considered the magnocellular neurons<sup>17,18</sup>. Therefore, in this study, the single neurons on coverslips with diameter >25 μm were classified as larger-sized neurons, which may largely represent the magnocellular neurons, while those with diameter <25 μm were classified as smaller-sized neurons, which may largely represent the parvocellular neurons. [Ca<sup>2+</sup>]<sub>i</sub> was measured by ratiometric fura-2 fluorescence imaging. Briefly, single neurons on coverslips were incubated with 2 μmol/l fura-2/AM (Dojin chemical, Kumamoto, Japan) for 40 min at room temperature, mounted in

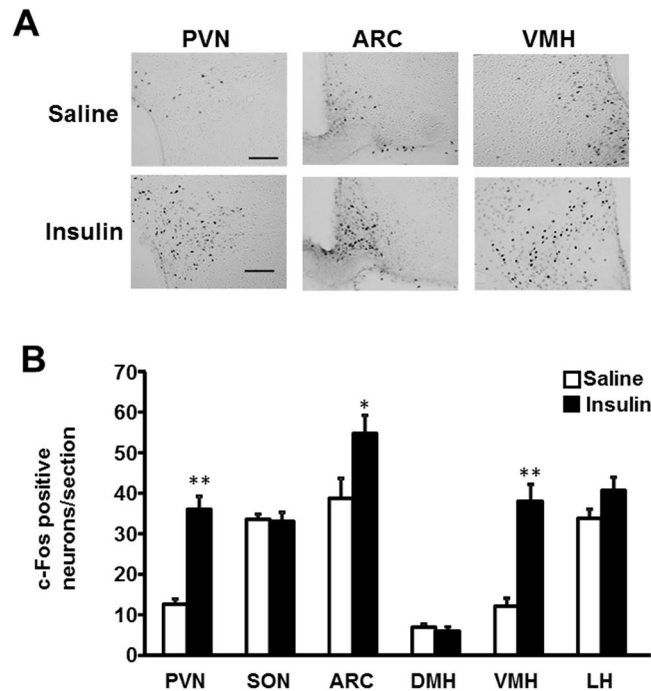


**Figure 1.** Effect of insulin on c-Fos expression in the hypothalamus. (A) Representative pictures showing c-Fos expression in the PVN, ARC and VMH of hypothalamus at 90 min after ICV injection of saline or insulin (100  $\mu$ U/2  $\mu$ l). Scale bar: 200  $\mu$ m. (B) Number of c-Fos-immunopositive (IR) neurons per section of the hypothalamic nuclei at 90 min after ICV injection of saline (white bars) or insulin (100  $\mu$ U/2  $\mu$ l) (black bars).  $n = 5$ . \*\* $p < 0.01$  and \* $p < 0.05$  vs. saline by one-way ANOVA followed by Tukey's test. Error bars are SEM.

chamber, and superfused with HEPES-buffered Krebs-Ringer bicarbonate buffer (HKRB) composed of (in mM) 129 NaCl, 5.0 NaHCO<sub>3</sub>, 4.7 KCl, 1.2 KH<sub>2</sub>PO<sub>4</sub>, 1.8 CaCl<sub>2</sub>, 1.2 MgSO<sub>4</sub>, 10 HEPES and 5.6 glucose at pH 7.4. The fluorescence images due to excitation at 340 and 380 nm were captured and ratio (F340/F380) images produced by Aquacosmos system (Hamamatsu Photonics, Hamamatsu, Japan). The single neurons subjected to [Ca<sup>2+</sup>]<sub>i</sub> measurements were subsequently immunostained for oxytocin using rabbit anti-oxytocin antibody (abcam, 1:1000) as previously described<sup>19</sup>.

**Statistical analysis.** Data are expressed as means  $\pm$  s.e.m. Data were analyzed for statistical significance by one-way ANOVA followed by Tukey's test.  $P < 0.05$  was considered significant.

## Results

ICV administration of insulin (100  $\mu$ U), compared to saline, significantly increased c-Fos expression in the PVN, arcuate nucleus (ARC) and ventromedial hypothalamus (VMH), but not SON, in the hypothalamus (Fig. 1A). Next, we performed double-staining for oxytocin and c-Fos in PVN after ICV insulin administration. The c-Fos immunoreactivity was observed in 25% and 38% of oxytocin neurons in PVN after ICV administration of saline and insulin, respectively (Fig. 2). Thus, insulin increased the incidence of the oxytocin neurons immunoreactive (IR) to c-Fos approximately by 13%. Furthermore, ICV insulin administration doubled the plasma oxytocin concentration (Fig. 3). These results indicated that insulin activates PVN oxytocin neurons *in vivo*.

To investigate whether insulin activates PVN oxytocin neurons by a direct action, we measured cytosolic calcium concentration ([Ca<sup>2+</sup>]<sub>i</sub>) in the single neurons isolated from PVN, followed by immunocytochemical identification of oxytocin neurons. Administration of insulin at 10<sup>-13</sup> M, 10<sup>-11</sup> M and 10<sup>-9</sup> M increased [Ca<sup>2+</sup>]<sub>i</sub> in the PVN neurons that were subsequently shown to be IR to oxytocin (Fig. 4A and B). Insulin at 10<sup>-13</sup> M increased [Ca<sup>2+</sup>]<sub>i</sub> with small amplitude in 6% of oxytocin-IR PVN neurons, and at 10<sup>-11</sup> M and at 10<sup>-9</sup> M it increased [Ca<sup>2+</sup>]<sub>i</sub> with larger amplitude in 18% of oxytocin-IR PVN neurons (Fig. 4D and E). Thus, insulin at 10<sup>-11</sup> M showed the maximal effect to increase [Ca<sup>2+</sup>]<sub>i</sub> in PVN oxytocin neurons. Furthermore, 14 of 24 insulin (10<sup>-11</sup> M)-responsive PVN neurons (53.8%) were IR to oxytocin (Fig. 4C), indicating that the oxytocin neuron is a major target for insulin in PVN. These results revealed that insulin directly activated oxytocin neurons and insulin action was maximal at 10<sup>-11</sup> M.

Activation of insulin receptors phosphorylates the insulin receptor substrate (IRS) proteins, which in turn activate phosphatidylinositol-3 kinase (PI3K), an enzyme that generates phosphatidylinositol-3, 4, 5-trisphosphate (PIP3). PIP3 activates 3-phosphoinositide-dependent protein kinase 1 (PDK1), which in turn activates protein kinase B (PKB, also known as Akt) and members of the atypical PKC family<sup>20</sup>. To investigate the role of PDK1 in the action of insulin in PVN oxytocin neurons, we generated the oxytocin neuron specific PDK1 knockout (*Oxy Pdk1* KO) mice. In the control *Oxy Cre* mice, expression of immunofluorescence for PDK1 was observed in oxytocin neurons in PVN, but absent in those neurons in *Oxy Pdk1* KO mice (Fig. 5). In *Oxy Cre* mice, ICV injection

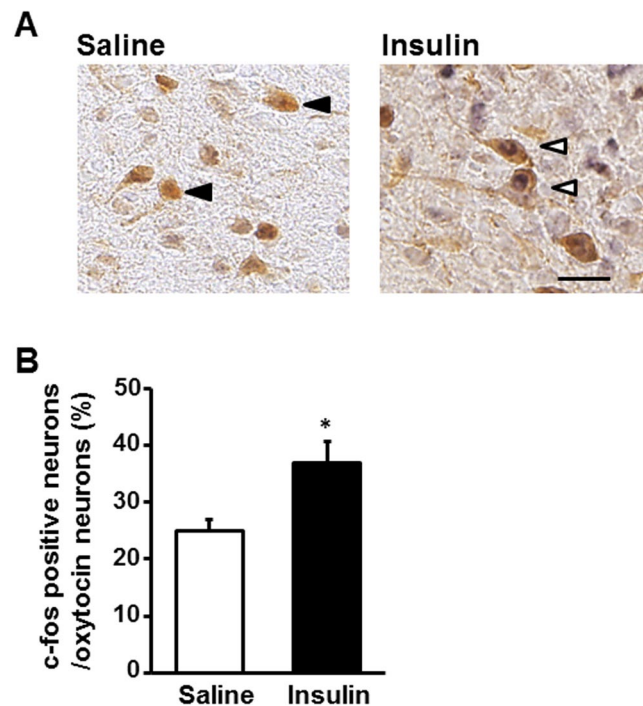


**Figure 2.** Effect of insulin on c-Fos expression in oxytocin-IR neurons. (A) Representative pictures depicting dual immunostaining for c-Fos and oxytocin in PVN after injection of saline or insulin ( $100\mu\text{U}/2\mu\text{l}$ ). Black arrowheads indicate oxytocin-IR neurons. White arrowheads indicate the neurons IR to both oxytocin and c-Fos. Scale bar:  $30\mu\text{m}$ . (B) Incidence of c-Fos-IR neurons in oxytocin-IR neurons.  $n = 5$ . \* $p < 0.05$  vs. saline by one-way ANOVA followed by Tukey's test. Error bars are SEM.

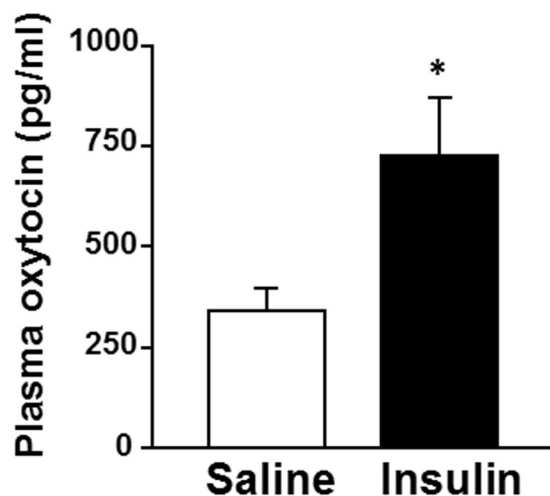


**Figure 3.** Effect of insulin on plasma oxytocin concentration. Plasma oxytocin concentrations at 30 min after ICV injection of saline or insulin ( $100\mu\text{U}/2\mu\text{l}$ ).  $n = 6-7$ . \* $p < 0.05$  vs. saline by one-way ANOVA followed by Tukey's test. Error bars are SEM.

of insulin ( $100\mu\text{U}$ ), compared to saline, markedly elevated the plasma oxytocin concentration at 30 minutes after injection (Fig. 6A). In *Oxy Pdk1* KO mice, in contrast, ICV injection of insulin failed to significantly alter plasma oxytocin at the same time point (Fig. 6B). These results suggest that the PDK1 in oxytocin neurons mediates the insulin action to stimulate oxytocin release.

We next examined whether insulin directly activates the larger-sized oxytocin neurons in PVN, which may represent magnocellular neurons, and if so, this action depends on PDK1. For this, we measured  $[\text{Ca}^{2+}]_i$  in single oxytocin neurons isolated from PVN of *Oxy Cre* mice and *Oxy Pdk1* KO mice. The oxytocin neurons with diameter of  $25\mu\text{m}$  or larger were defined as larger-sized neurons. Insulin at  $10^{-11}\text{M}$  interacted with and increased  $[\text{Ca}^{2+}]_i$  in the larger-sized oxytocin neurons of *Oxy Cre* mice (Fig. 7A,C,D). The  $[\text{Ca}^{2+}]_i$  increase with substantial

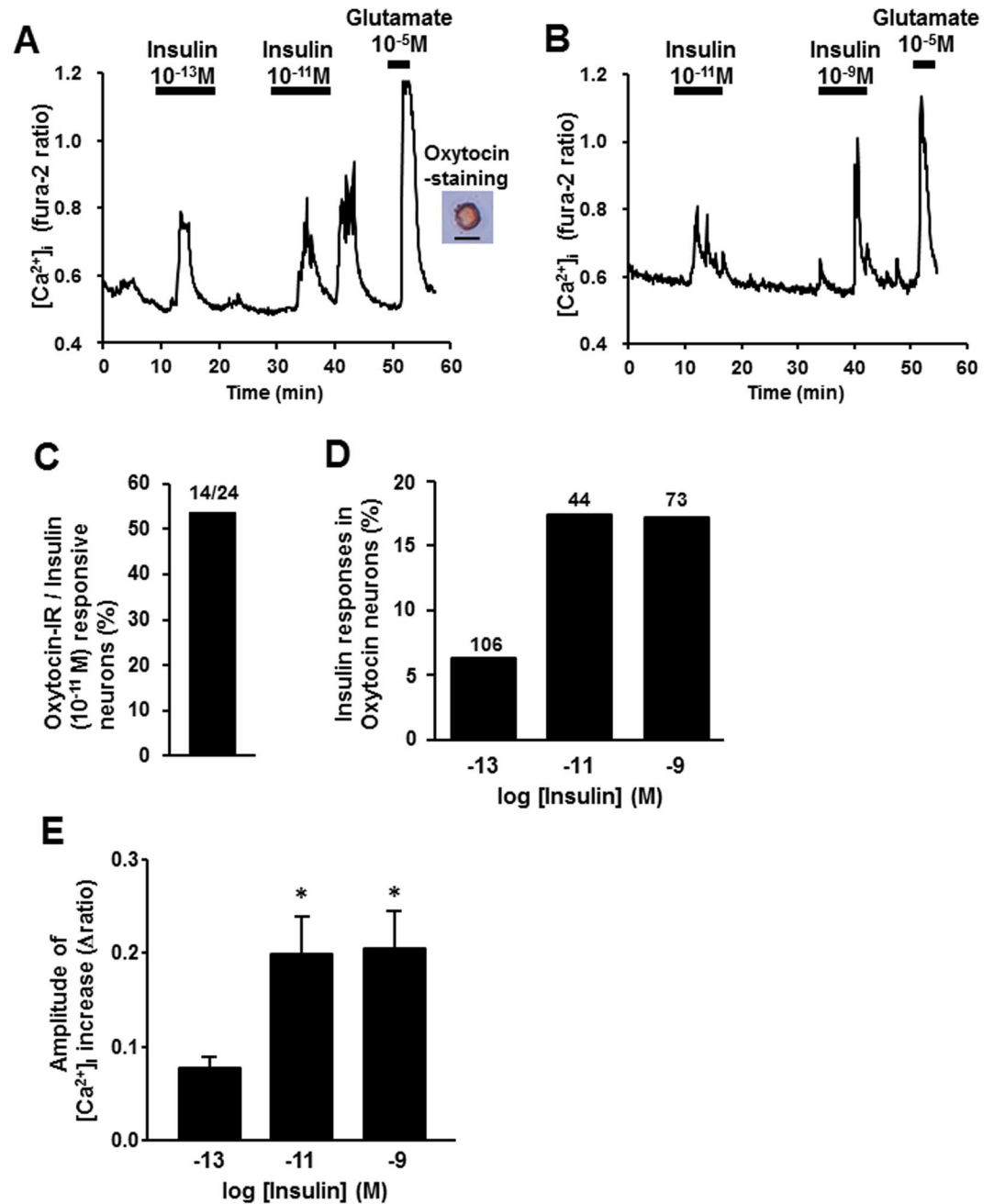


**Figure 4.** Insulin increases  $[Ca^{2+}]_i$  in single PVN oxytocin neurons. (A) Insulin at  $10^{-13}$  M and  $10^{-11}$  M increased  $[Ca^{2+}]_i$  (left panel) in a single PVN neuron that was subsequently shown to be IR to oxytocin (right panel). Scale bar is  $25\ \mu\text{m}$ . (B) Insulin at  $10^{-11}$  and  $10^{-9}$  M increased  $[Ca^{2+}]_i$  in a single PVN neuron. (C) 14 of 24 (53.8%) neurons that responded to insulin were IR to oxytocin. (D) Incidence of  $[Ca^{2+}]_i$  responses to insulin in PVN oxytocin neurons, expressed by percentage. Numbers around each point indicate the number of PVN oxy neurons. (E) Average amplitude of insulin-induced  $[Ca^{2+}]_i$  increases ( $\Delta\text{ratio}$ ) in oxytocin neurons. \* $p < 0.05$  vs. basal level by one-way ANOVA followed by Tukey's test. Error bars are SEM.

amplitude occurred in about 27% of larger-sized oxytocin neurons from *Oxy Cre* mice. In contrast,  $10^{-11}$  M insulin increased  $[Ca^{2+}]_i$  only in 7% of those neurons from *Oxy Pdk1* KO mice (Fig. 7B,C,D). Thus, the ability of insulin to increase  $[Ca^{2+}]_i$  in larger-sized oxytocin neurons was markedly diminished in *Oxy Pdk1* KO mice (Fig. 7A–D). These results indicated that insulin activates the larger-sized oxytocin neuron of PVN via the signaling pathway involving Pdk1. In contrast, the smaller-sized ( $<25\ \mu\text{m}$ ) parvocellular oxytocin neurons from *Oxy Cre* mice and those from *Oxy Pdk1* KO mice equally responded to insulin (Fig. 8A and B): both incidence and amplitude of  $[Ca^{2+}]_i$  increases in smaller-sized neurons in response to insulin were not significantly different between *Oxy Cre* and *Oxy Pdk1* KO mice (Fig. 8C and D).



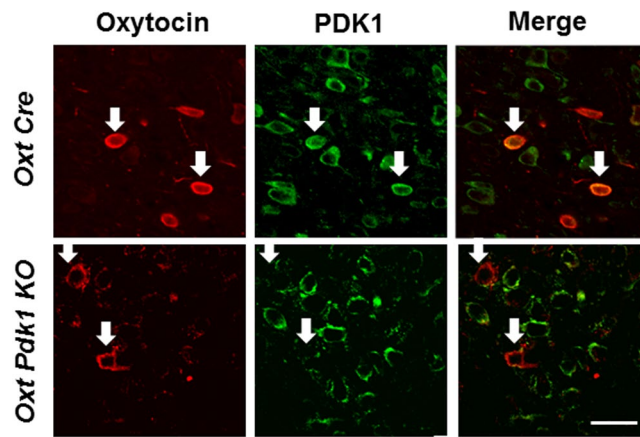


**Figure 5.** Double immunostaining for oxytocin and PDK1 in PVN of *Oxy Cre* and *Oxy Pdk1 KO* mice. Double immunostaining for oxytocin and PDK1 in PVN. The upper rows show *Oxy Cre* mice and the lower rows *Oxy Pdk1 KO* mice. Left: oxytocin (Red: Alexa 594 fluorescence), middle: PDK1 (Green: Alexa 488), right: merged images. Scale bar: 30  $\mu$ m. White arrows: oxytocin-IR neurons.

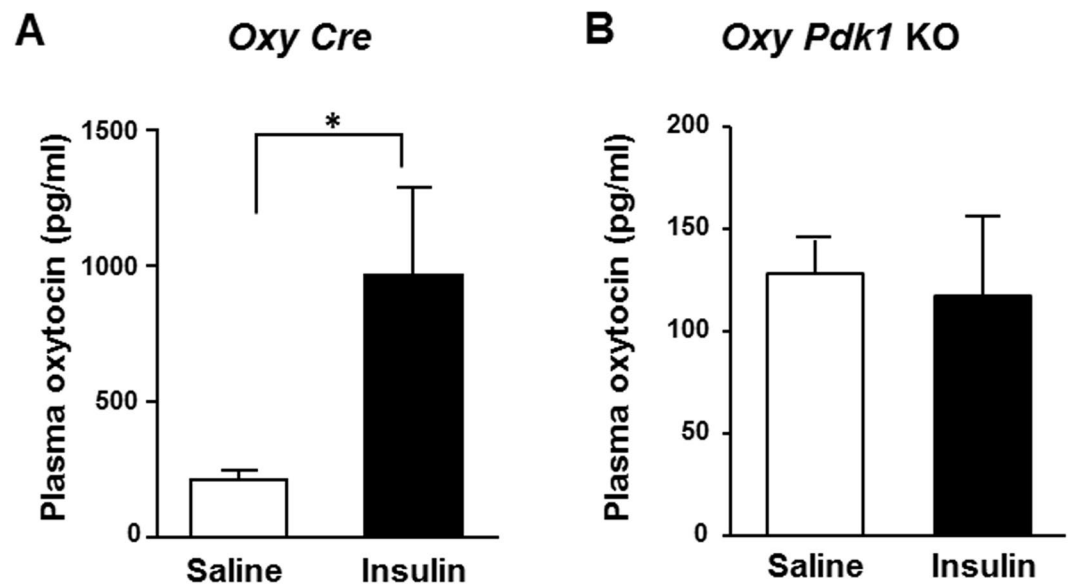


**Figure 6.** Insulin fails to increase plasma oxytocin concentrations in *Oxy Pdk1 KO* mice. Plasma oxytocin concentrations at 30 min after ICV injection of saline or insulin (100  $\mu$ U/2  $\mu$ l) in *Oxy Cre* mice (A) and *Oxy Pdk1 KO* mice (B). n = 6. \*p < 0.05 vs. saline by one-way ANOVA followed by Tukey's test. Error bars are SEM.

## Discussion

In this study, we found that insulin directly interacts with the larger-sized PVN oxytocin neurons to increase  $[Ca^{2+}]_i$  via signaling involving PDK1 and that this neuronal activation is relayed to oxytocin release in circulation. The present study has identified the PVN oxytocin neuron as a novel and substantial target for the central action of insulin.

In the brain as well as peripheral tissues, PDK1, the downstream of PI 3-kinase, serves as a key molecule in insulin signaling cascade. It has previously been shown that PDK1 is implicated in the  $[Ca^{2+}]_i$  responses to various stimuli in both AgRP/NPY and POMC neurons in the arcuate nucleus (ARC)<sup>21–23</sup>. We here showed that the insulin action to promote the activity of PVN larger-sized oxytocin neurons and oxytocin release were blunted in *Oxy Pdk1 KO* mice. These results reveal a critical role of PDK1 in the PVN larger-sized oxytocin neurons, which couples the central insulin action to the neuronal activity and release of oxytocin. It has recently been reported that insulin promotes oxytocin release from SON oxytocin neurons via PI-3 kinase signaling<sup>24</sup>. This previous and our current studies taken together suggest that insulin induces oxytocin release through the PI 3-kinase-PDK1 pathway.

Although insulin can pass through the blood brain barrier, the insulin concentration in the cerebrospinal fluid is reportedly much lower than that in the plasma, producing a large concentration difference greater than 10 times in humans<sup>25,26</sup>. Transportation of insulin to the cerebrospinal fluid is slow, and little influenced by

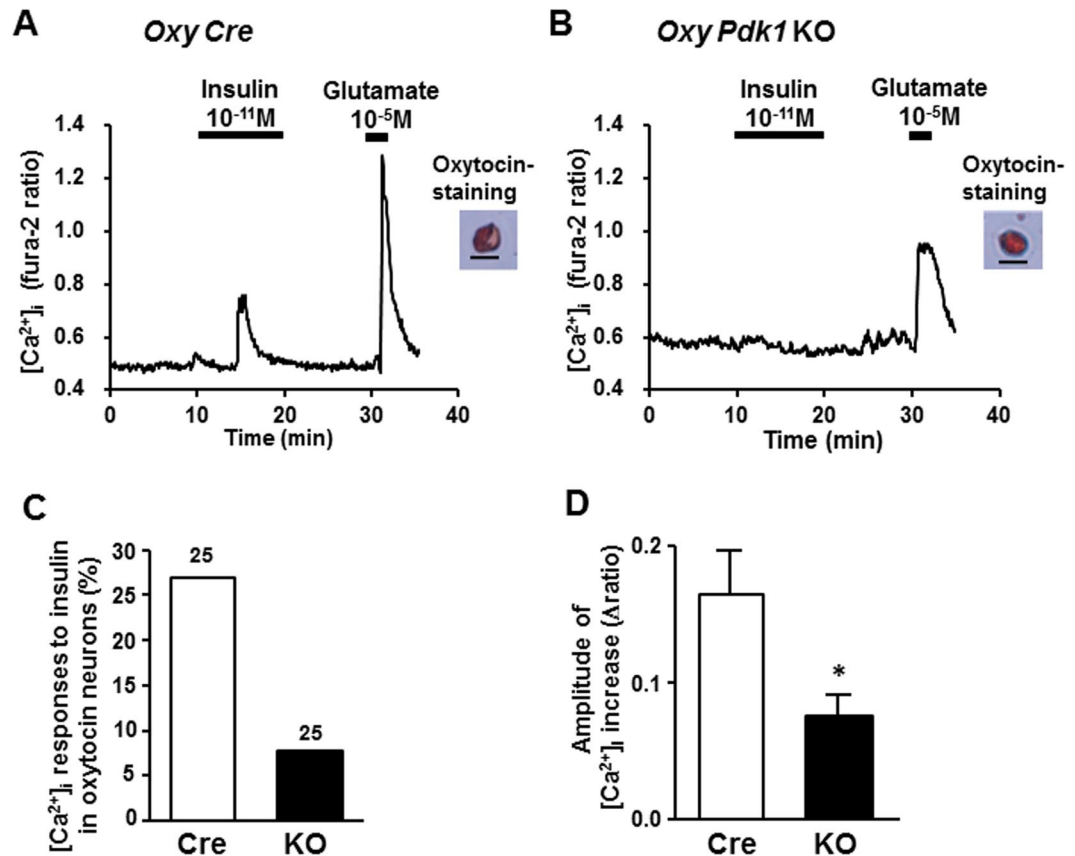


**Figure 7.** Insulin fails to substantially increase  $[Ca^{2+}]_i$  in larger-sized oxytocin neurons of PVN in *Oxy Pdk1* KO mice. (A,B) Representative  $[Ca^{2+}]_i$  responses to  $10^{-11}$  M insulin in larger-sized oxytocin neurons of PVN, possibly representing magnocellular neurons, isolated from *Oxy Cre* mice (A) and *Oxy Pdk1* KO mice (B). Single neurons with diameter  $>25.0\ \mu\text{m}$  were classified as larger-sized neurons in this study. These neurons from both mice similarly responded to  $10^{-5}$  M glutamate. (C) Incidence of  $[Ca^{2+}]_i$  responses to insulin in PVN oxytocin neurons, expressed by percentage. Numbers around each point indicate the number of PVN oxy neurons. (D) Average amplitude of  $[Ca^{2+}]_i$  responses to insulin ( $\Delta\text{ratio}$ ) in oxytocin neurons. Scale bar:  $25\ \mu\text{m}$ . \* $p < 0.05$  vs. *Oxy Cre* mice by one-way ANOVA followed by Tukey's test. Error bars are SEM.

dietary property in humans<sup>27,28</sup>. The insulin concentration in human cerebrospinal fluid at fasting condition is  $<10\ \text{pmol/L}$  ( $10^{-11}$  M), a level that is too low to activate the insulin receptor in peripheral tissues. Surprisingly, from the analysis of isolated neurons in the current study, the PVN oxytocin neurons are activated by insulin at the concentrations as low as  $10^{-13}$  to  $10^{-11}$  M. This finding supports that the PVN oxytocin neurons can be activated by the low levels of insulin present in cerebrospinal fluid. The mechanism that renders the PVN oxytocin neurons responsive to these low concentrations of insulin remains to be elucidated. However, the sensitivity of single PVN oxytocin neurons to insulin could be increased by 5 mM glucose present in superfusion solution in the current  $[Ca^{2+}]_i$  measurement. It was reported that the SON oxytocin neuron is activated by co-administration of glucose (5 mM) and insulin. We previously reported that insulin and glucose synergistically increased  $[Ca^{2+}]_i$  in PVN nesfatin-1 neurons<sup>29</sup>. Therefore, oxytocin neurons, when primed with high glucose concentration, may be activated by the levels of insulin present in cerebrospinal fluid after meal.

The plasma concentrations of oxytocin are significantly decreased in obese and diabetic patients<sup>16,30–32</sup>. Moreover, expression and plasma concentration of oxytocin also decreased in obese model animals<sup>14,30,32</sup>. The insulin resistance in the brain as well as peripheral tissues occurs in obese subjects and animals<sup>32–35</sup>. The present finding that ICV injection of insulin promotes oxytocin secretion suggest that insulin resistance in oxytocin neurons could serve as a factor that leads to the reduction in oxytocin concentrations in obese and/or type 2 diabetic patients.

Recently oxytocin, besides its physiological function in parturition and lactation, also regulate appetite and metabolism<sup>36–39</sup>. Intranasal administration of oxytocin in humans has been reported to ameliorate overeating<sup>39–43</sup> and ameliorates hyperglycemia<sup>44</sup>. Moreover, ICV injection of oxytocin decreases food intake in both normal-weight and obese animals<sup>14,45</sup>. Furthermore, oxytocin enhances energy expenditure, a centrally-regulated function<sup>46</sup>. Thus, the beneficial effects of oxytocin on body weight regulation largely depend on the central action. In the present study, insulin activated the PVN parvocellular, as well as magnocellular, oxytocin neurons that project to several brain regions. It was suggested that PVN parvocellular oxytocin neurons play a role in central action of insulin to regulate energy metabolism. We furthermore found that insulin increases  $[Ca^{2+}]_i$  in

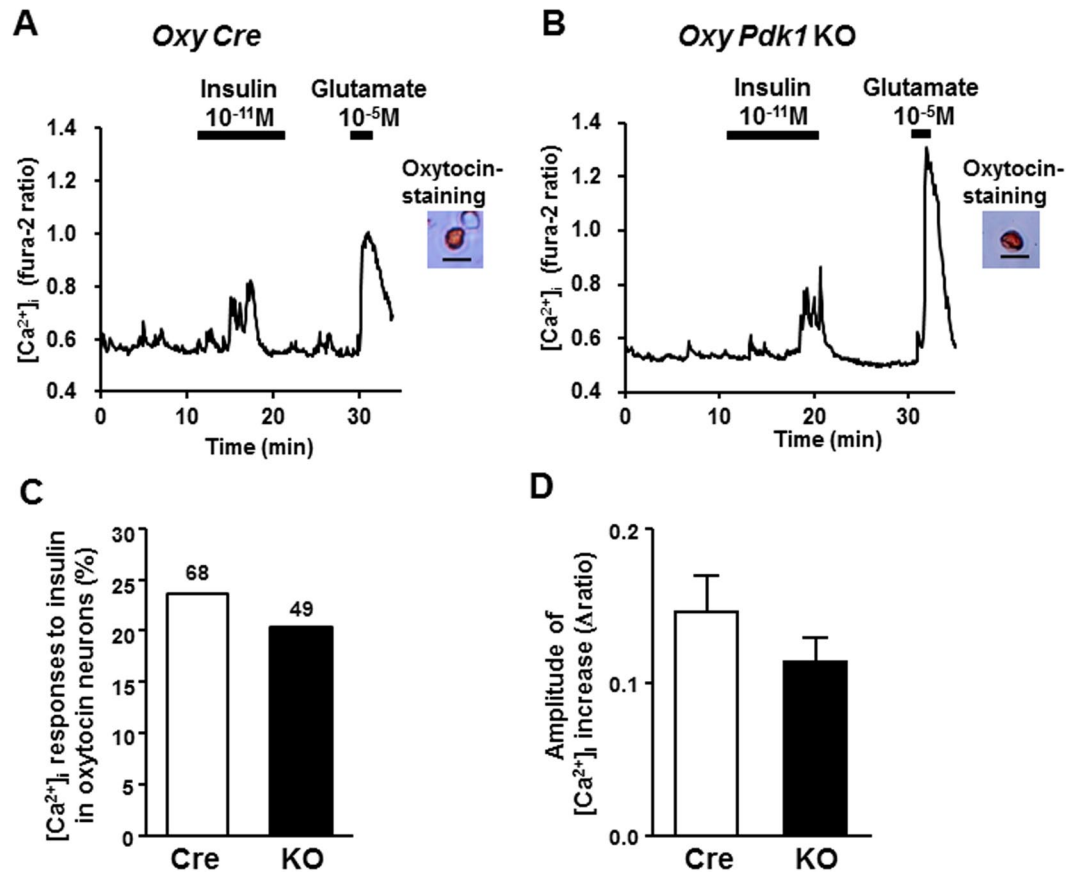


**Figure 8.** Insulin increases  $[Ca^{2+}]_i$  in smaller-sized oxytocin neurons of PVN. (A,B) Representative  $[Ca^{2+}]_i$  responses to  $10^{-11}$  M insulin in smaller-sized oxytocin neurons of PVN, possibly representing parvocellular neurons, isolated from *Oxy Cre* mice (A) and *Oxy Pdk1 KO* mice (B). Single neurons with diameter  $<25.0 \mu\text{m}$  were classified as smaller-sized neurons in this study. (C) Incidence of  $[Ca^{2+}]_i$  responses to insulin in PVN oxytocin neurons, expressed by percentage. Numbers around each point indicate the number of PVN oxy neurons. (D) Average amplitude of  $[Ca^{2+}]_i$  responses to insulin ( $\Delta\text{ratio}$ ) in oxytocin neurons examined. Scale bar:  $25 \mu\text{m}$ .

the PVN smaller-sized oxytocin neurons, which may largely represent their parvocellular subpopulation, in a PDK1-independent manner, being contrasted to the PDK1-dependent action in the larger-sized magnocellular oxytocin neurons. This finding suggests the signaling pathway-dependent sorting of insulin-induced multiple oxytocin functions. Further studies are required to further elucidate the insulin signaling mechanisms in the PVN parvocellular and magnocellular oxytocin neurons and their link to specific functions, which could help utilize a specific branch of the insulin-oxytocin axis for treating obesity, diabetes and/or perinatal disorders.

## References

- Obici, S., Zhang, B. B., Karkaniyas, G. & Rossetti, L. Hypothalamic insulin signaling is required for inhibition of glucose production. *Nat Med* **8**, 1376–1382 (2002).
- Inoue, H. *et al.* Role of hepatic STAT3 in brain-insulin action on hepatic glucose production. *Cell Metab* **3**, 267–275 (2006).
- Havrankova, J., Roth, J. & Brownstein, M. Insulin receptors are widely distributed in the central nervous system of the rat. *Nature* **272**, 827–829 (1978).
- Brüning, J. C., Gautam, D. & Burks, D. J. Role of brain insulin receptor in control of body weight and reproduction. *Science* **289**, 2122–2125 (2002).
- Sarnyai, Z. & Kovács, G. L. Oxytocin in learning and addiction: From early discoveries to the present. *Pharmacol Biochem Behav* **119**, 3–9 (2014).
- Robinson, D. A. *et al.* Oxytocin mediates stress induced analgesia in adult mice. *J Physiol* **540**, 593–606 (2002).
- Ferguson, J. N. *et al.* Social amnesia in mice lacking the oxytocin gene. *Nat Genet* **25**, 284–288 (2000).
- Gil, M., Bhatt, R., Picotte, K. B. & Hull, E. M. Sexual experience increases oxytocin receptor gene expression and protein in the medial preoptic area of the male rat. *Psychoneuroendocrinology* **38**, 1688–1697 (2013).
- Donaldson, Z. R. & Young, L. J. Oxytocin, vasopressin, and the neurogenetics of sociality. *Science* **322**, 900–904 (2008).
- Bartz, J. A. *et al.* Effects of oxytocin on recollections of maternal care and closeness. *Proc Natl Acad Sci USA* **107**, 21371–21375 (2010).
- Camerino, C. Low sympathetic tone and obese phenotype in oxytocin-deficient mice. *Obesity* **17**, 980–984 (2009).
- Takayanagi, Y. *et al.* Oxytocin receptor-deficient mice developed late-onset obesity. *Neuroreport* **19**, 951–955 (2008).
- Zhang, G. *et al.* Neuropeptide exocytosis involving synaptotagmin-4 and oxytocin in hypothalamic programming of body weight and energy balance. *Neuron* **69**, 523–535 (2011).



14. Zhang, G. & Cai, D. Circadian intervention of obesity development via resting-stage feeding manipulation or oxytocin treatment. *Am J Physiol Endocrinol Metab* **301**, E1004–1012 (2011).
15. Wu, Z. L. *et al.* An obligate role of oxytocin neurons in diet induced energy expenditure. *Plos One* **7**, e45167 (2012).
16. Qian, W. *et al.* Increased circulating levels of oxytocin in obesity and newly diagnosed type 2 diabetic patients. *J Clin Endocrinol Metab* **99**, 4683–4689 (2014).
17. Tasker, J. G. & Dudek, F. E. Electrophysiological properties of neurones in the region of the paraventricular nucleus in slices of rat hypothalamus. *J Physiol* **434**, 271–293 (1991).
18. Hoffman, N. W., Tasker, J. G. & Dudek, F. E. Immunohistochemical differentiation of electrophysiologically defined neuronal populations in the region of the rat hypothalamic paraventricular nucleus. *J Comp Neurol* **307**, 405–416 (1991).
19. Maejima, Y. *et al.* Nesfatin-1-regulated oxytocinergic signaling in the paraventricular nucleus causes anorexia through a leptin-independent melanocortin pathway. *Cell Metab* **10**, 355–365 (2009).
20. Matsumoto, M. *et al.* Inhibition of insulin-induced activation of Akt by a kinase-deficient mutant of the epsilon isoform of protein kinase C. *J Biol Chem* **276**, 14400–14406 (2001).
21. Cao, Y. *et al.* PDK1-Foxo1 in agouti-related peptide neurons regulates energy homeostasis by modulating food intake and energy expenditure. *Plos One* **6**, e18324 (2011).
22. Sasanuma, H., Nakata, M., Parmila, K., Nakae, J. & Yada, T. PDK1-FoxO1 pathway in AgRP neurons of arcuate nucleus promotes bone formation via GHRH-GH-IGF1 axis. *Mol Metab* **6**, 428–439 (2017).
23. Iskandar, K. *et al.* PDK-1/FoxO1 pathway in POMC neurons regulates Pomc expression and food intake. *Am J Physiol Endocrinol Metab* **298**, E787–798 (2010).
24. Song, Z., Levin, B. E., Stevens, W. & Sladek, C. D. Supraoptic oxytocin and vasopressin neurons function as glucose and metabolic sensors. *Am J Physiol Regul Integr Comp Physiol* **306**, R447–456 (2014).
25. Strubbe, J. H., Porte, D. Jr. & Woods, S. C. Insulin responses and glucose levels in plasma and cerebrospinal fluid during fasting and refeeding in the rat. *Physiol Behav* **44**, 205–208 (1988).
26. Kern, W. *et al.* Low cerebrospinal fluid insulin levels in obese humans. *Diabetologia* **49**, 2790–2792 (2006).
27. Wallum, B. J. *et al.* Cerebrospinal fluid insulin levels increase during intravenous insulin infusions in man. *J Clin Endocrinol Metab* **64**, 190–194 (1987).
28. Schwartz, M. W. *et al.* Kinetics and specificity of insulin uptake from plasma into cerebrospinal fluid. *Am J Physiol* **259**, E378–E383 (1990).
29. Gantulga, D., Maejima, Y., Nakata, M. & Yada, T. Glucose and insulin induce Ca<sup>2+</sup> signaling in nesfatin-1 neurons in the hypothalamic paraventricular nucleus. *Biochem Biophys Res Commun* **420**, 811–815 (2012).
30. Coiro, V. *et al.* Oxytocin response to insulin-induced hypoglycemia in obese subjects before and after weight loss. *J Endocrinol Invest* **11**, 125–128 (1988).
31. Kujath, A. S. *et al.* Oxytocin levels are lower in premenopausal women with type 1 diabetes mellitus compared with matched controls. *Diabetes Metab Res Rev* **31**, 102–112 (2015).
32. De Souza, C. T. *et al.* Consumption of a fat-rich diet activates a proinflammatory response and induces insulin resistance in the hypothalamus. *Endocrinology* **146**, 4192–4199 (2005).
33. Thaler, J. P. *et al.* Obesity is associated with hypothalamic injury in rodents and humans. *J Clin Invest* **122**, 153–162 (2012).
34. Puig, J. *et al.* Hypothalamic damage is associated with inflammatory markers and worse cognitive performance in obese subjects. *J Clin Endocrinol Metab* **100**, E276–E281 (2015).
35. Cazettes, F., Cohen, J. I., Yau, P. L., Talbot, H. & Convit, A. Obesity-mediated inflammation may damage the brain circuit that regulates food intake. *Brain Res* **1373**, 101–109 (2011).
36. Altirriba, J. *et al.* Divergent effects of oxytocin treatment of obese diabetic mice on adiposity and diabetes. *Endocrinology* **155**, 4189–4201 (2014).
37. Maejima, Y. *et al.* Peripheral oxytocin treatment ameliorates obesity by reducing food intake and visceral fat mass. *Aging* **3**, 1169–1177 (2011).
38. Morton, G. J. *et al.* Peripheral oxytocin suppresses food intake and causes weight loss in diet-induced obese rats. *Am J Physiol Endocrinol Metab* **302**, E134–144 (2012).
39. Zhang, H. *et al.* Treatment of obesity and diabetes using oxytocin or analogs in patients and mouse models. *Plos One* **8**, e61477 (2013).
40. Lawson, E. A. *et al.* Oxytocin reduces caloric intake in men. *Obesity* **23**, 950–956 (2015).
41. Ott, V. *et al.* Oxytocin reduces reward-driven food intake in humans. *Diabetes* **62**, 3418–3425 (2013).
42. Thienel, M. *et al.* Oxytocin's inhibitory effect on food intake is stronger in obese than normal-weight men. *Int J Obes* **40**, 1707–1714 (2016).
43. Maejima, Y. *et al.* Nasal oxytocin administration reduces food intake without affecting locomotor activity and glycemia with c-Fos induction in limited brain areas. *Neuroendocrinology* **101**, 35–44 (2015).
44. Klement, J. *et al.* Oxytocin Improves  $\beta$ -Cell Responsivity and Glucose Tolerance in Healthy Men. *Diabetes* **66**, 264–271 (2017).
45. Nakata, M. *et al.* Paraventricular NUCB2/Nesfatin-1 Supports Oxytocin and Vasopressin Neurons to Control Feeding Behavior and Fluid Balance in Male Mice. *Endocrinology* **157**, 2322–2332 (2016).
46. Kasahara, Y. *et al.* Oxytocin receptor in the hypothalamus is sufficient to rescue normal thermoregulatory function in male oxytocin receptor knockout mice. *Endocrinology* **154**, 4305–4315 (2013).

## Acknowledgements

The authors thank Dr. Bradford B Lowell at Beth Israel Deaconess Medical Center/Harvard Medical School for providing Oxytocin Cre transgenic mice. We also thank Ms. Megumi Motoshima and Ms. Atsumi Shinozaki for technical assistance. This study was supported by CREST, JST to M.K. A part of this study was supported by Grant-in-Aid for Scientific Research (C) (15K09442 & 18K11028) (M.N.) and for Challenging Exploratory Research (26670453) (T.Y.) from Japan Society for the Promotion of Science (JSPS). A part of this work was supported by Ministry of Education, Culture, Sports, Science and Technology of Japan (MEXT)-Supported Programs for Strategic Research Foundation at Private Universities 2013–2017 to T.Y. This study was supported by Grant from Daiichi-Sankyo Co. (T.Y. and M.N.). This study was subsidized by JKA through its promotion funds from KEIRIN RACE to T.Y.

## Author Contributions

B.Z., M.N. and T.Y. designed experiments. B.Z. and M.N. conducted experiments and analyzed data. B.Z., M.N., T.Y. prepared the manuscript. J.N. and W.O. generated transgenic mice. All authors evaluated and approved the manuscript.

## Additional Information

**Competing Interests:** The authors declare no competing interests.

**Publisher's note:** Springer Nature remains neutral with regard to jurisdictional claims in published maps and institutional affiliations.



**Open Access** This article is licensed under a Creative Commons Attribution 4.0 International License, which permits use, sharing, adaptation, distribution and reproduction in any medium or format, as long as you give appropriate credit to the original author(s) and the source, provide a link to the Creative Commons license, and indicate if changes were made. The images or other third party material in this article are included in the article's Creative Commons license, unless indicated otherwise in a credit line to the material. If material is not included in the article's Creative Commons license and your intended use is not permitted by statutory regulation or exceeds the permitted use, you will need to obtain permission directly from the copyright holder. To view a copy of this license, visit <http://creativecommons.org/licenses/by/4.0/>.

© The Author(s) 2018